Vγ9Vδ2 T cells strengthen cisplatin inhibition activity against breast cancer MDA-MB-231 cells by destructing mitochondrial function and cell ultrastructure

Xin Huang[1*1], Cunchuan Wang[1], Ningxia Wang[1]

Abstract

Background: Breast cancer ranks second of new cases and fifth of death in 2018 world widely. Chemotherapy, one of cancer therapeutic strategies, plays important role in controlling mortality of breast cancer. Cis-platinum (CDDP), one of traditional chemotherapy drugs, had been used clinically for years. The crucial limitation of CDDP is due to its adverse effects on immune system. Development of new protocol that can minimize side effect and meanwhile elevate clinical efficacy of traditional drug like CDDP will eventually benefit cancer patients. Vγ9Vδ2 T cells had been reported to be able to up-regulate immune function of cancer patients, therefore, our hypothesis is that introduction of Vγ9Vδ2 T cells could potentiate CDDP efficacy against breast cancer.

Methods: In the present work, breast cancer cell line MDA-MB-231 was used a model cell to test our hypothesis. The therapeutic dose of CDDP in vitro was analyzed by flow cytometry; The cytoskeleton was visualized by using a confocal microscopy, and the ultrastructure of the membrane was observed by atomic force microscopy to observe the effect of combined action on MDA-MB-231 cells; The mitochondrial function of MDA-MB-231 cells was detected, and the relevant mechanism of Vγ9Vδ2 T in enhancing cisplatin cells' inhibition of MDA-MB-231 cells was discussed.

Results: Vγ9Vδ2 T cells could enhance CDDP-induced MDA-MB-231 cell membrane ultrastructure disorder and cytoskeleton disorder, and enhance the inhibition of CDDP on MDA-MB-231 cells, of which Vγ9Vδ2 T cells enhancing CDDP-induced mitochondrial dysfunction was one of its mechanisms.

Conclusion: In this study，the mechanism of Vγ9Vδ2 T cells in enhancing the inhibition of cisplatin on MDA-MB-231 cells was studied, which could provide an important scientific clue for developing effective treatment schemes for breast cancer, especially the refractory TNBC

[1] Correspondence:1072083306@qq.com
1 Department of Breast Surgery, The First Affiliated Hospital of Jinan University, 613 West Huangpu Road, Guangzhou 510630, Guangdong, People's Republic of China
Full list of author information is available at the end of the article

breast cancer, based on Vγ9Vδ2 T cells in the future.
Key words: Vγ9Vδ2 T cell；cisplatin；MDA-MB-231 cells；inhibitory effect

Background

Breast cancer is one of leading causes of cancer death in women world widely. Currently, clinical treatments against breast cancer mainly include surgery, chemotherapy, radiotherapy, endocrine and molecularly targeted therapy. Among these protocols, chemotherapy is commonly used in clinical for breast cancer treatment. Although chemotherapy drug contributed a lot to treat tumor patients, the severe side effects and disadvantages should not be underestimated. For instance, previous literature reported that chemotherapy drugs can generate pro-tumorigenic and pro-metastatic effects, which contributes to cancer recurrence and resistance to anti-tumor therapy [1]. It's also reported the chemotherapy could promote cancer cell evolution through engulfing senescent or early-apoptotic cells [2]. In one word, there is increasingly scientific evidences revealing the evil part of chemotherapy drugs in tumor treatment, including promotions of metastasis, proliferation, immune escape, and so on [1-3]. Therefore, to develop new treatment strategy including nanotechnology-based methodologies [4-9] for cancer has been under continuous investigation during the past a few years. One of the most highlighted progresses is the successful achievement of complete remission in clinical of B cell lymphoma after treated with chimeric antigen receptor (CAR) T cells [10-13]. This set a new paradigm for cancer treatment using immune cells.

Vγ9Vδ2 T cells belongs to one subset of human peripheral γδ T cells that are one of two components of T lymphocytes. Vγ9Vδ2 T cells had been shown promising clinical value because of the potent anti-tumor activity [14, 15]. Previously, published reports had revealed that Vγ9Vδ2 T cells could be developed into a new strategy for cancer immunotherapy [16-19]. For example, Hiranmoy Das et al reported that Vγ9Vδ2 T cells could inhibit breast cancer cell proliferation by regulating crucial molecules related to cell survival and apoptosis [20]; the mice model study by Philippe Clezardin et al discovered that Vγ9Vδ2 T cells exerted promising breast tumor inhibition activity in the context of zoledronic acid pre-treatment [21]; notably, clinical Phase I trial study on breast cancer patients revealed that sustained population of Vγ9Vδ2 T cells were positively correlated with sound prognosis [22]. Therefore, previous reports altogether indicated that Vγ9Vδ2 T cells-based immunotherapy will be one of promising therapeutic

approach for breast cancer [18, 23-26]. In this work, we proposed a new protocol by combining chemotherapy drug cis-platinum (CDDP) and cytotoxic immune cell (Vγ9Vδ2 T cell) to treat a selected breast cancer model cell line MDA-MB-231, and tried to reveal the in vitro efficacy of this combination from the single cell level by applying microscopy methodologies. It should be noted here that CDDP has been used clinically to treat breast cancer for many years, and the side effects include severe impairments on immune function of patients. Therefore, combination of these two treatments, CDDP and Vγ9Vδ2 T cells, could provide us new insights into developments of creative anti-tumor strategy.

In the present work, we attempted to study whether or not the combination of CDDP and Vγ9Vδ2 T cells could generate the most optimal cytotoxicity against breast cancer cell MDA-MB-231 from both large-scale number of cells as well as single cell level. We used flow cytometry, atomic force microscopy and confocal microscopy to examine mitochondrial function, cell ultrastructure and cytoskeletal organization, we found that, comparing with single treatment alone, CDDP plus Vγ9Vδ2 T cells exhibited significant greater inhibition against MDA-MB-231 cell growth, elevated mitochondrial dysfunction, ultrastructural and cytoskeletal impairments, implicated with Vγ9Vδ2 T cells could potentiate CDDP inhibition activity against breast cancer cell MDA-MB-231. Altogether, our present work will promote development of new clinical treatment protocol for breast cancer and eventually benefit cancer patients.

Materials and methods

γδ T cell isolation and culture

The methodology of γδ T cell isolation and culture had been described in detail in previous reports [14, 27, 28]. Briefly, the isolated peripheral blood monocyte cells (PBMCs) using Ficoll-Paque centrifuge from healthy volunteers were cultured in RPMI-1640 culture medium supplemented with 10% fetal bovine serum (FBS), IL-2 (5ng/ml) and zoledronate (10 nM); then cells were seeded into 24 or 48 well-plates. After cultured for 10-12 days, the expanded Vγ9Vδ2 T cells were used to conduct experiments. The purity of Vγ9Vδ2 T cells was assayed using flow cytometry, and only those exceeded 90% of purity were used in our experiments.

MDA-MB-231 cell viability assay

Breast cancer cell line MDA-MB-231 (MDA-MB-231, Tam1, ATCC® CRL-3435™) was used as a cell model in our work. Cells were cultured in RPMI-1640 culture medium containing 10% BSA, and cells were used for experiments after the confluency reached 70-80%. For cis-platinum (CDDP) treatment, three CDDP dosages include 120 μM, 240 μM, and 480 μM were used, and treatment times of 24 hours and 48 hours were applied. For γδ T cell treatment, γδ T cell number was determined according to effector (γδ T): target (MDA-MB-231) ratios (1:1, 5:1, and 10:1), the 6 hours of cell-cell interaction was applied here. As for combined treatments, MDA-MB-231 cells were firstly treated with CDDP (240 μM) for 24 hours, followed T cell incubation (5:1) for 6 hours after cells were twice washed to remove extra CDDP. Then MDA-MB-231 cells were collected and stained with Propidium Iodide (PI) for 5 min at room temperature, and flow cytometry was used to analyze the dead cell percentage.

Mitochondrial function assay of MDA-MB-231 cells

To analyze mitochondrial function of MDA-MB-231 cells in the presence and absence of CDDP or γδ T cells, mitochondrial ROS detection assay kit (Sigma), MitoTracker (Thermofisher) staining and mitochondrial membrane potential assay kit (Sigma) were applied in our work, and sample preparation procedures referred to the standard protocols provided by the reagent providers. Afterward, cells were analyzed by flow cytometry. All obtained data by flow cytometry were further analyzed with FlowJo (FLOWJO, LLC) software.

Atomic force microscope visualization of membrane ultrastructure

To visualize membrane surface nanostructures, atomic force microscopy (AFM) (Bioscope Catalyst, Bruker) was applied to scan single MDA-MB-231 cells. The detailed methodology for AFM principle and sample preparation could be detailed referred in previous published works [29-35]. In brief, the tapping mode AFM was used to scan cells at room temperature in air. The spring constant of the cantilever was calibrated at 0.06 ~ 0.11 N/m. The average roughness (R_a) that describes topography properties of membrane surface was obtained according to the following formula [32]:

$$R_a = \frac{1}{N} \cdot \sum_{n=1}^{N} \left| z_n - \bar{z} \right|$$

where N represents the total number of data points in a selected area, z_n is the height of the n^{th} point and $\bar{z}$ is the mean height.

Cytoskeleton visualization using confocal microscopy imaging

To achieve cytoskeleton (F-actin and tubulin-α) visualization, fluorescence staining was performed by following Invitrogen standard immunofluorescence staining protocol. Staining was performed at room temperature. FITC-phalloidin was used to stain actin, and mouse anti-human fluorescent tubulin- α antibody was used to stain tubulin-α. Cell nucleus was stained with dye DAPI. Cells were washed with PBS between each step, then anti-fade reagent was added before performing confocal analyses. The confocal microscopy system used in our work was Leica SP8, and 60X oil immersed objective was applied for imaging.

Data analyses and statistics

All statistical results were expressed as mean±SEM (Standard Error of the Mean). To analyze statistical significance between experimental groups and control group, one-way ANOVA was applied to compare the difference between the control group and each experimental group. Statistical significance: ns, no significance; *, $p<0.05$; **, $P<0.01$; ***, $P<0.001$; ****, $P<0.0001$.

Results

Both cis-Platinum and γδ T cells inhibited MDA-MB-231 viability in a dose-dependent manner

To determine inhibition concentration of cis-platinum and incubation time with MDA-MB-231 cells, we firstly used flow cytometry to analyze cell viability in the presence of cis-platinum (**FIG. 1A**). The analyzed results showed that, for 24 hours of incubation, 120 μM of cis-platinum did not inhibit cell viability statistically, whereas 240 μM and 480 μM could induce cell death significantly, from 1.29±0.13 (control, %) to 21.47±1.79 (%) and 97.4±0.72 (%), respectively. As for 48 hours of incubation, the percentage of cell death increased from 1.7±0.12 (control) to 41.13±1.68 and 98.1±0.7 after incubated with 240 μM and 480 μM of cis-platinum, respectively (**FIG. 1B**). Furthermore, we conducted killing assay to analyze the inhibiting efficacy of Vγ9Vδ2 T cells against MDA-MB-231 cells, and results were shown in **Figure 1**(**C-D**). It indicated that when the ratio of effector (Vγ9Vδ2 T cells): target (MDA-MB-231) reached at 5:1, the inhibition efficacy (24±1.53, %) against MDA-MB-231 could be significantly higher than the control group (2.67±0.9, %) (**FIG. 1D**) after 6 hours of co-incubation. Moreover, the inhibition efficacy increased to 38.33 ± 2.4% for the E:T=10:1 group. These results altogether indicated that both cis-platinum and γδ T cells inhibited MDA-MB-231 viability in a dose-dependent manner.

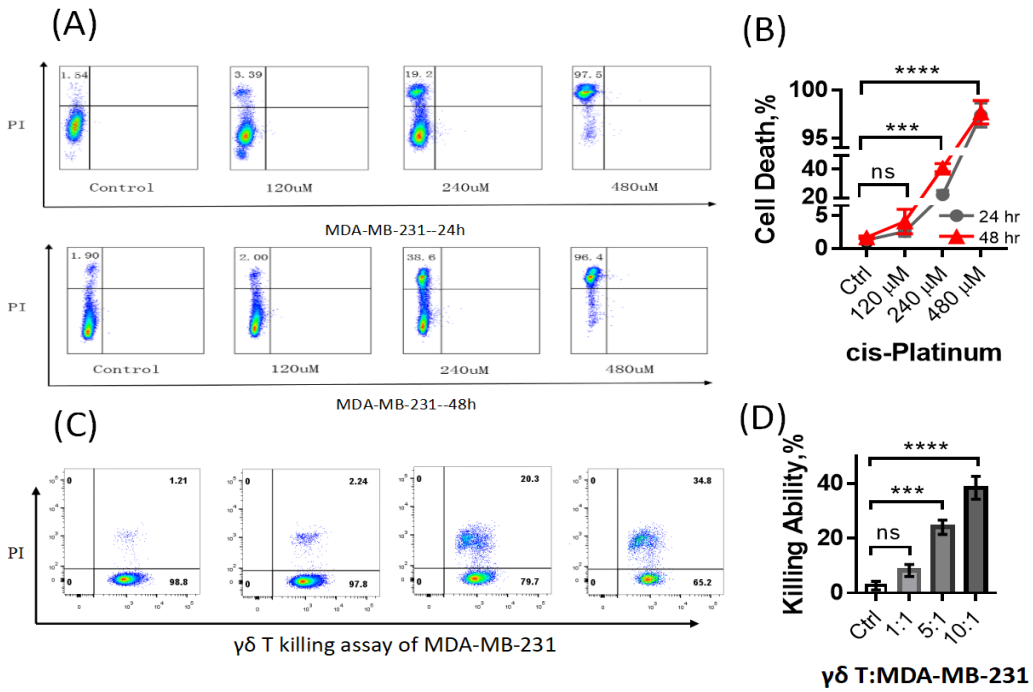

Figure 1. Cell viability and killing assay of MDA-MB-231 cells in the presence of cis-platinum (CDDP) and Vγ9Vδ2 T cells. (A) Representative flow cytometry graphs of cell death detection of MDA-MB-231 cells. (B) Statistical graph of MDA-MB-231 cell viability in the absence and presence of CDDP, showing CDDP induced cell death in a dose-dependent manner. (C, D) Killing assay results of MDA-MB-231 cells by Vγ9Vδ2 T cells. ns, no significance; ***, P<0.001; ****, P<0.0001.

γδ T cells could strength cis-Platinum inhibition activity against MDA-MB-231

Furthermore, we tried to check whether or not the combination of cis-platinum (CDDP) and γδ T cells could exert stronger inhibiting efficacy than one alone. According to results shown in **Figure 1**, since 120 μM cis-platinum failed to statistically inhibit cell viability but 480 μM cis-platinum killed >97% cells, we thus selected 240 μM as work concentration and 24 hours as incubation time for cis-platinum, and 5:1 as effector: target for γδ T cells. We found that the combination of cis-platinum and γδ T cells could significantly elevate the inhibition against MDA-MB-231 compared with the control group as well as CDDP alone (**FIG. 2A**). Specifically, the inhibition percentage of MDA-MB-231 for control group and CDDP was 6±1.15 and 21±1.53, respectively, whereas 37±2.65 for combination group (**FIG. 2B**). Together, the present results implied that combination had significant superiority compared with CDDP alone or γδ T cells alone.

Combination of γδ T cells and cis-Platinum dramatically suppressed ROS production

Given one of inhibition mechanism of cis-platinum (CDDP) against breast cancer cells is to destruct mitochondrial respiration and metabolism, we thus detected mitochondrial alterations of MDA-MB-231 in the context of CDDP and γδ T cell treatment. Here, we analyzed the reactive oxygen species (ROS) of MDA-MB-231 using flow cytometry (**FIG. 2C**). The statistics showed that ROS production significantly decreased after cells treated with either CDDP or γδ T cells, from 73.7±2.22 (control) to 47.5±3.82 (CDDP) and 31.17±2.05, and CDDP plus γδ T cells further decreased ROS production to 8.92±1.67 (**FIG. 2D**). Such results suggested mitochondrial function of MDA-MB-231 cells were impaired in the presence of CDDP, γδ T cells and their combination could further aggravate such impairment.

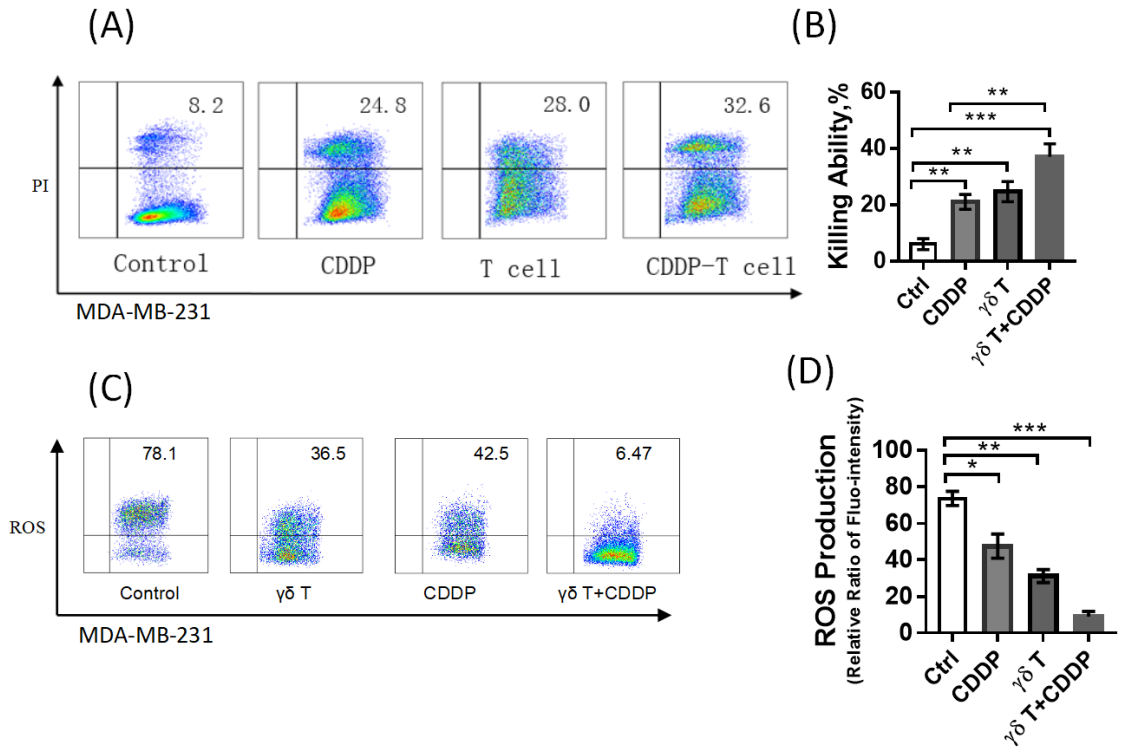

Figure 2. (A) Flow cytometry plot analyses of MDA-MB-231 cell viability in the context of treatment of cis-platinum (CDDP) plus Vγ9Vδ2 T cells, showing data of one time of experiment. (B) Statistical data from triple repetitions of experiments, showing that Vγ9Vδ2 T cells could significantly strengthen CDDP cytotoxicity against MDA-MB-231. (C) Flow cytometry plot data of reactive oxygen species (ROS) production from one time of experiment. (D) Triple repetitions, clearly indicating that Vγ9Vδ2 T cells could dramatically strengthen CDDP-induced reduction of ROS production of in MDA-MB-231 cells. *, p<0.05; **, P<0.01; ***, P<0.001.

Combination of γδ T cells and cis-Platinum induced the most significant loss of mitochondrial mass and membrane potential

Because both CDDP and γδ T cells could reduce ROS production in MDA-MB-231, it's of interest to further reveal how mitochondrial function were damaged. We therefore investigated changes of mitochondrial mass and mitochondrial membrane potential using flow cytometry plus fluorescence labelling, and results were shown as **Figure 3**. **Figure 3A** showed representative flow cytometry graphs of mitochondrial mass of fluorescence dye MitoTracker pre-labelled MDA-MB-231 cells. According to statistical analyses. (**FIG. 3B**), we could easily see that both γδ T cells and CDDP plus γδ T cells significantly reduced mitochondrial mass in MDA-MB-231 cells by ~25%. Furthermore, we analyzed

membrane potential of mitochondria in MDA-MB-231, which is one of the most important indicators of mitochondrial function. We discovered that the membrane potential was dramatically suppressed to approximate 75% of the control in the presence of CDDP or γδ T cells, and combination of CDDP and γδ T cells decreased it to ~50% of the control group (**FIG. 3C**). These results altogether indicated mitochondrial function was inhibited in the presence of CDDP, γδ T cells, and CDDP plus γδ T cells induced the most significant loss of mitochondrial mass and membrane potential in MDA-MB-231 cells.

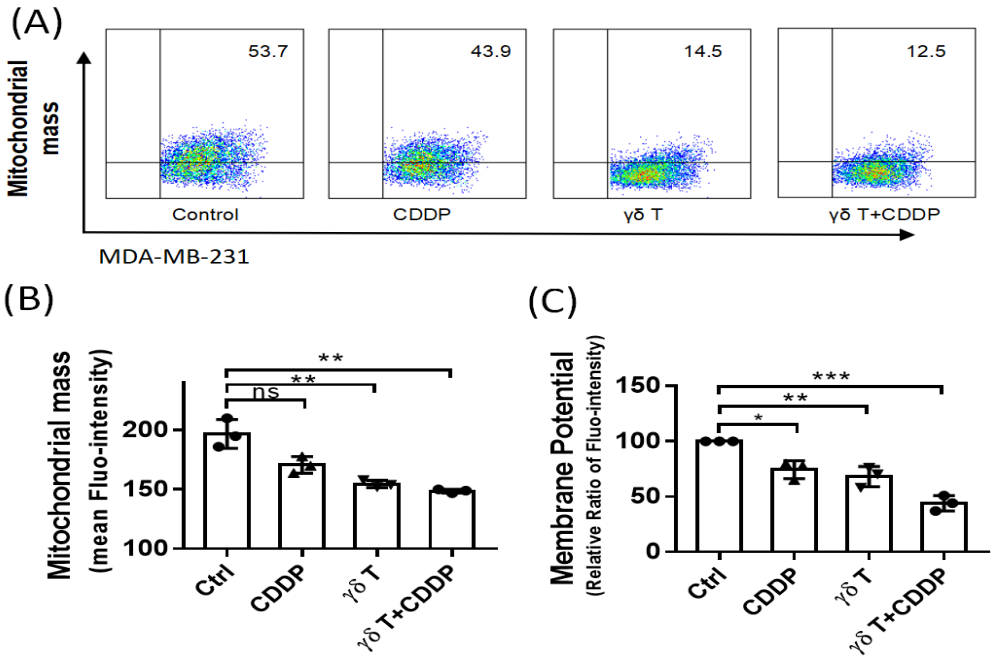

Figure 3. Vγ9Vδ2 T cells apparently potentiated CDDP-induced mitochondrial dysfunction including mitochondrial mass and membrane potential. (A) Representative flow cytometry graphs. (B) Statistical graph of loss of mitochondrial mass in the context of treatments. (C) Statistical graph of loss of mitochondrial membrane potential. ns, no significance; *, p<0.05; **, P<0.01; ***, P<0.001.

γδ T cells potentiated destruction of MDA-MB-231 membrane nanostructures induced by cis-Platinum

To exert inhibition effects to MDA-MB-231 growth, cis-platinum (CDDP) uptake by MDA-MB-231 cells or cell-cell interaction between γδ T and MDA-MB-231 cells is required. Therefore, the earliest alteration in MDA-MB-231 might occurred on cell membrane. This made it of importance to detect ultrastructural changes in the context of treatments. We thus used atomic force microscopy (AFM) to visualize and

analyze the potential alterations of MDA-MB-231 cell membrane, and results are shown in **Figure 4**. (**Figure 4A)** showed topography images of single MDA-MB-231 cells, no obvious changes could be identified from these images. We further scanned membrane surface ultrastructure, and found that membrane integrity tended to be impaired, particularly for cells treated with CDDP plus γδ T cells (**FIG. 4B**). Since membrane surface average roughness is one of optimal parameters for describing membrane surface topography, it was statistically analyzed (**FIG. 4C**). We found that membrane surface roughness was significantly elevated after cells treated with both CDDP and γδ T cells. For CDDP plus γδ T cell treated group, the roughness was elevated to 13.43 ± 0.26 nm from 9.67 ± 0.3 nm of the control group (**FIG. 4C**). Therefore, AFM visualization and analyses indicated that γδ T cells could further potentiate destruction of MDA-MB-231 membrane nanostructures induced by cis-Platinum.

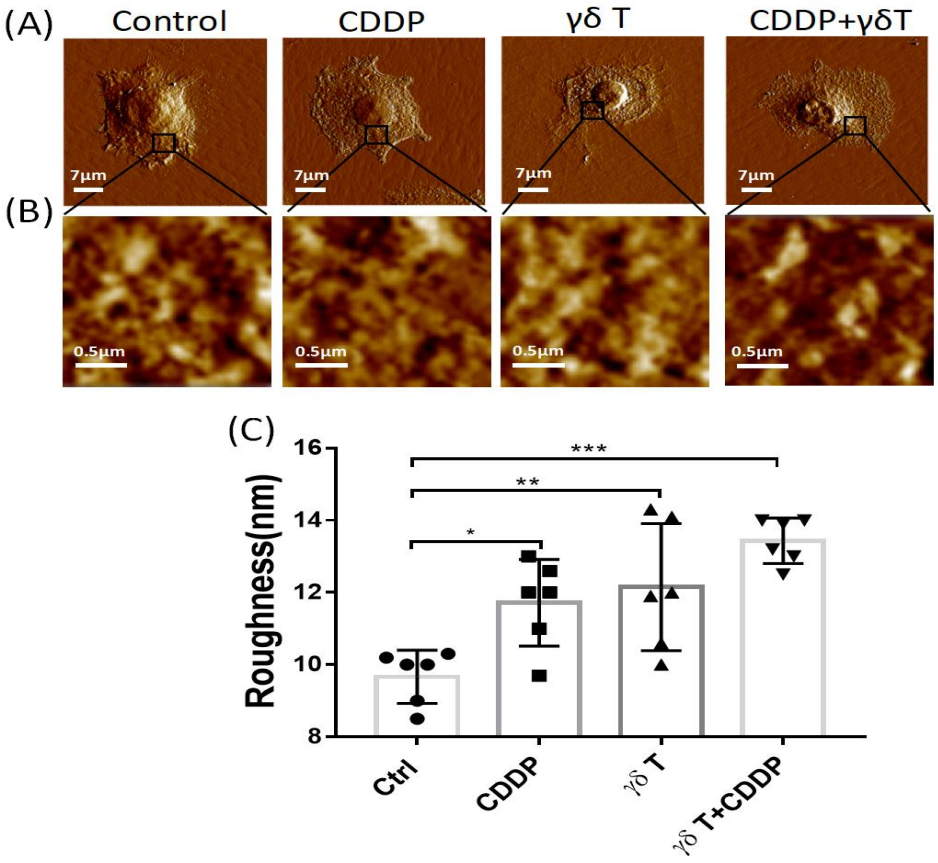

Figure 4. Atomic force microscopy (AFM) visualization of membrane surface ultrastructure of MDA-MB-231 cells. (A) Representative topography images of single cells, scanning size: 70 μm. (B) Membrane surface nanostructure images zoomed in from corresponding images in (A), scanning size: 2 μm. (C) Statistical comparison of surface average roughness. *, $p<0.05$; **, $P<0.01$; ***, $P<0.001$.

Combination of γδ T cells and cis-Platinum destructed MDA-MB-231 cytoskeleton the most significantly

Since cytoskeleton plays crucial roles in the multiple biological processes, including cell shape, migration, motility, mitosis, cell-cell communication and signal transduction and so on, it's necessary to evaluate how the cytoskeleton structures of MDA-MB-231 was impacted in the context of CDDP or γδ T cell treatment. Here, we applied confocal microscopy and flow cytometry to visualize and quantify cytoskeletal alterations, as shown in **Figure 5**. For untreated cells, we could clearly see the actin (green fluorescence), one of main cytoskeletal components, appeared to be filamentous and well-organized; as for tubulin, another main cytoskeletal component, mainly localized at polar sites of cells (**FIG. 5A**). However, after MDA-MB-231 cells were treated with CDDP (**FIG. 5B**) or γδ T cells (**FIG. 5C**), the cytoskeletal structures were destructed, the fluorescence became dimmed and the filamentous structures could not be distinguished clearly. As for combination of CDDP and γδ T cells, both cytoskeletal components actin and tubulin were completely damaged, as evidenced by loss of fluorescence signal (**FIG. 5D**). Moreover, flow cytometry was also used to confirm confocal results, as it can provide statistical analyses based on a large number of cells. From the flow cytometry results (**FIG. 5E**), we could clearly tell that both CDDP and γδ T cells could destruct the cytoskeletal organization of MDA-MB-231 cells, and combination of γδ T cells and cis-Platinum destructed MDA-MB-231 cytoskeleton the most significantly.

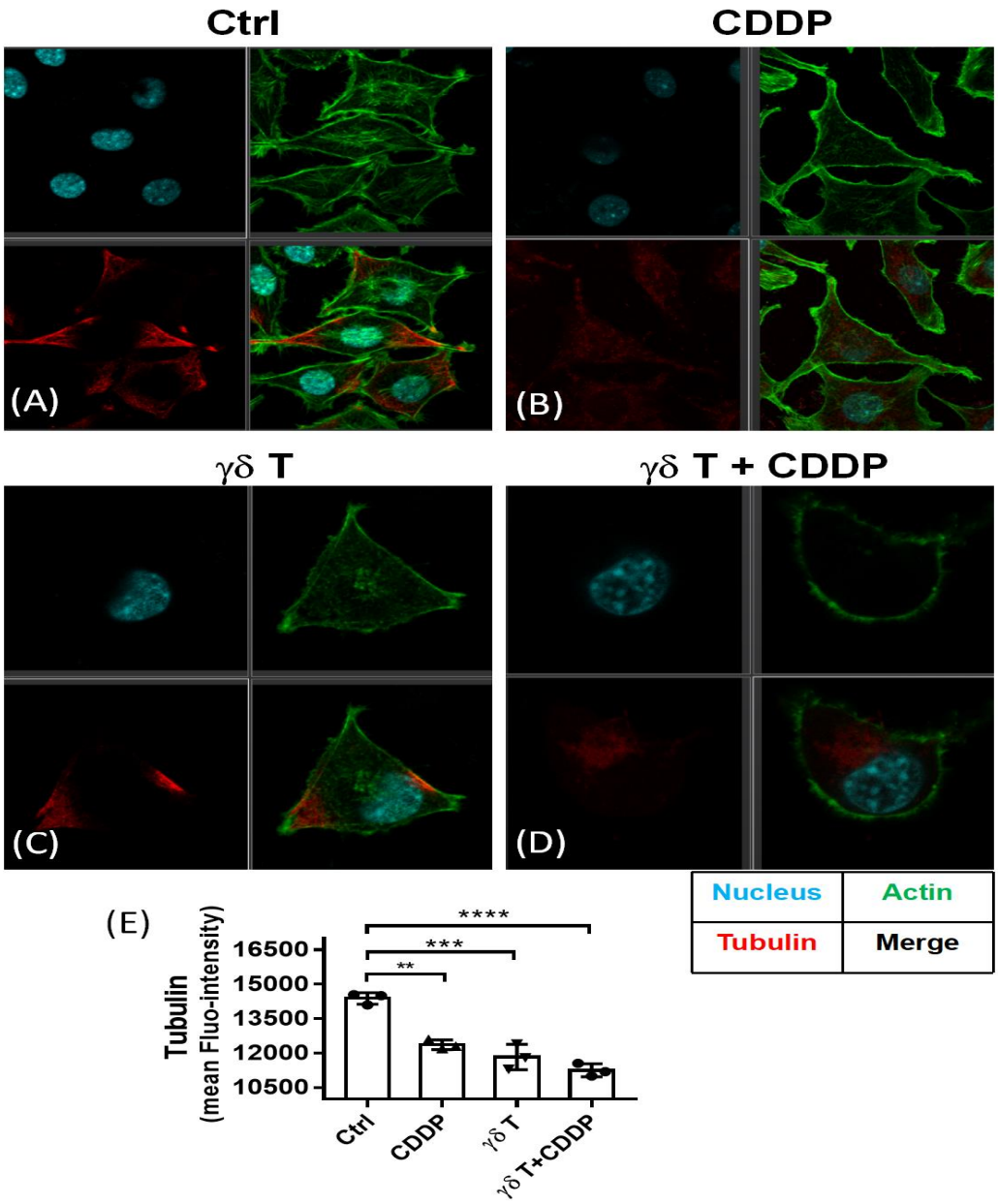

Figure 5. Confocal microscopy visualization of cytoskeleton. (A-D) Cytoskeletal changes in the absence and presence of CDDP, Vγ9Vδ2 T cells and CDDP plus Vγ9Vδ2 T cells were visually detected by Leica SP8 laser scanning confocal microscopy. (E) Quantification analyses of tubulin content of MDA-MB-231 cells in the context of treatments by flow cytometry. **, P<0.01; ***, P<0.001; ****, P<0.0001.

Discussion

Cis-platinum has been used as clinical therapy drug against breast cancer for many years, however, its severe side effects limited the treatment efficacy clinically. Vγ9Vδ2 T cell has been increasingly recognized as new therapy strategy for cancer, since this cell could regulate immune function of the patients [14]. Although immune cells-based immunotherapy for tumor has been highlighted as a new research and development direction world widely, the clinical value of chemotherapy drug-based traditional protocol could not be under estimated. Therefore, how to combine these two different kinds of treatment protocols to achieve the maximal benefits to cancer patients needs extensive investigations.

In the present work, we for the first time attempted to combine Vγ9Vδ2 T cells and cis-platinum (CDDP) to treat breast cancer MDA-MB-231 cells, and flow cytometry, atomic force microscopy and confocal microscopy were used to analyze the inhibit efficacy from the multiple and single cell views. We firstly discovered that 240 μM of CDDP had similar inhibition ability (~20%) against MDA-MB-231 cells as 5:1 of γδ T: MDA-MB-231. This indicated either chemotherapy drug alone or Vγ9Vδ2 T cell alone might not be optimal way to efficiently inhibit the cancer cell growth, because the inhibition rate against MDA-MB-231 cells was only around 20% for both treatments. However, the combination of CDDP and Vγ9Vδ2 T cells could more significantly suppress cancer cell viability, the killing rate of cancer cells elevated up to ~40%. This result suggested the synergetic effects of cisplatin with Vγ9Vδ2 T cells for the inhibition of breast cancer viability. These results could be implicated with two interpretations, one is that γδ T cells could strength cis-Platinum inhibition activity against breast cancer cell MDA-MB-231; the other one is that pretreatment using the chemotherapy drug cis-platinum made MDA-MB-231 became more sensitive to γδ T cells. Nevertheless, the present results implied that combination had significant superiority compared with CDDP alone or γδ T cells alone.

One of the major difficulties for tumor to be completely suppressed in clinical lies that cancer cells could produce large amount of reactive oxygen species (ROS) due to their rapid growth, which results from out of balance of redox homeostatic state (mild pro-oxidative state) [36-38]. This is one of reasons why cancer cells, particularly tumor microenvironment, could suppress the immune responses of cytotoxic immune cells. In this context, reduction in ROS production could be implicated with impairment of

mitochondrial function in the presence of CDDP or γδ T cell treatment. Our research results evidenced that MDA-MB-231 cells treated with CDDP or γδ T cells could significantly reduce not only mitochondrial mass but also mitochondrial membrane potential. The loss of mitochondrial membrane potential leads to cell apoptosis and cell death eventually. This explained why treatments of MDA-MB-231 cells by CDDP, γδ T cells, or their combination led to decreases in ROS production as well. Nevertheless, our work exhibited that γδ T cells could further potentiate CDDP inhibition against breast cancer cell MDA-MB-231, and the induced impairments in mitochondrial function played crucial role in this process.

After investigations at the scale of large number of cells, further work from the single cell view would provide us new knowledge on understanding how γδ T cells potentiated CDDP inhibition against MDA-MB-231 cells. The practicable nanobiotechnology, atomic force microscopy, could present new angle at the single cell level to reveal the veil on how cell membrane surface nanostructures were altered in the context of treatments. In our results, we discovered that alterations of membrane nanostructures induced by CDDP or γδ T cells were not visually apparent, however, further statistical analyses based on average roughness revealed gradual loss of membrane intact nanostructures in the context of treatments. Furthermore, cytoskeletal destructions suggested that CDDP or γδ T cell treatment impaired cytoskeleton organization more significantly than membrane surface ultrastructure. These visualized observations from the single cell level implied that cytoskeleton would be more sensitive indicator than membrane ultrastructure for revealing growth inhibition of MDA-MB-231 cells in the context of anti-tumor drug or cytotoxic immune cells. Additionally, both ultrastructural and cytoskeletal visualizations suggested that γδ T cells could further strengthen cytotoxicity of CDDP against breast cancer cell MDA-MB-231, implicating with the great clinical value to supplement γδ T cells to the current chemotherapy protocols to benefit tumor patients eventually.

Conclusion

The present work for the first time demonstrated an in vitro paradigm for combining cis-platinum and γδ T cells to treat breast cancer cells, which clearly showed that γδ T cells could greatly strengthen cisplatin inhibition activity against breast cancer MDA-MB-231 cells. Our results revealed that mitochondrial

dysfunction, cell membrane ultrastructural destruction and cytoskeleton disorganization together contributed to the growth inhibition of MDA-MB-231 cells.

Abbreviations

CDDP: Cis-platinum; PBMCs: Peripheral blood monocyte cells; FBS: Fetal bovine serum; AFM: Atomic force microscopy; ROS: Reactive oxygen species

Availability of data and materials

The datasets generated/analyzed during the current study are available.

Authors' contributions

Xin Huang and Ningxia Wang designed the experiments; Xin Huang conducted experiments; Xin Huang and Cunchuan Wang provided research materials and methods; Xin Huang analyzed data; Xin Huang wrote the manuscript. All authors read and approved the final manuscript.

Acknowledgements

Not applicable.

Competing interests

The authors declare that they have no competing interests.

Availability of data and materials

We declared that materials described in the manuscript, including all relevant raw data, will be freely available to any scientist wishing to use them for noncommercial purposes, without breaching participant confidentiality.

Ethics approval and consent to participate

Not applicable.

Consent for publication

All authors consent for publication.

Funding

Not applicable.

Author details

1 Department of Breast Surgery, The First Affiliated Hospital of Jinan University, 613 West Huangpu Road, Guangzhou 510630, Guangdong, People's Republic of China.

.

References

1. Shaked, Y., *Balancing efficacy of and host immune responses to cancer therapy: the yin and yang effects.* Nat Rev Clin Oncol, 2016. **13**(10): p. 611-26.
2. Tonnessen-Murray, C.A., et al., *Chemotherapy-induced senescent cancer cells engulf other cells to enhance their survival.* J Cell Biol, 2019. **218**(11): p. 3827-3844.
3. Rodier, F., et al., *Persistent DNA damage signalling triggers senescence-associated inflammatory cytokine secretion.* Nat Cell Biol, 2009. **11**(8): p. 973-9.
4. Kannan, K., et al., *Facile fabrication of CuO nanoparticles via microwave-assisted method: photocatalytic, antimicrobial and anticancer enhancing performance.* International Journal of Environmental Analytical Chemistry, 2020: p. 1-14.
5. Prabakaran, S., et al., *Polymethyl methacrylate–ovalbumin @ graphene oxide drug carrier system for high anti-proliferative cancer drug delivery.* Applied Nanoscience, 2019. **9**(7): p. 1487-1500.
6. Praphakar, R.A., et al., *A pH-sensitive guar gum-grafted-lysine-beta-cyclodextrin drug carrier for the controlled release of 5-flourouracil into cancer cells.* J Mater Chem B, 2018. **6**(10): p. 1519-1530.
7. Rajan, M., et al., *Poly-carboxylic acids functionalized chitosan nanocarriers for controlled and targeted anti-cancer drug delivery.* Biomed Pharmacother, 2016. **83**: p. 201-211.
8. Vinothini, K., et al., *Dual Role of Lanthanum Oxide Nanoparticles Functionalized Co-Polymeric Micelle for Extended Anti-Cancer Drug Delivery.* ChemistrySelect, 2019. **4**(18): p. 5206-5213.
9. Jeyaraj, M., et al., *Surface functionalization of natural lignin isolated from Aloe barbadensis Miller biomass by atom transfer radical polymerization for enhanced anticancer efficacy.* RSC advances, 2016. **6**(56): p. 51310-51319.
10. Magee, M.S. and A.E. Snook, *Challenges to chimeric antigen receptor (CAR)-T cell therapy for cancer.* Discov Med, 2014. **18**(100): p. 265-71.
11. Neelapu, S.S., et al., *Chimeric antigen receptor T-cell therapy - assessment and management of toxicities.* Nat Rev Clin Oncol, 2018. **15**(1): p. 47-62.
12. Tran, E., D.L. Longo, and W.J. Urba, *A Milestone for CAR T Cells.* N Engl J Med, 2017. **377**(26): p. 2593-2596.
13. Brudno, J.N. and J.N. Kochenderfer, *Chimeric antigen receptor T-cell therapies for lymphoma.* Nat Rev Clin Oncol, 2018. **15**(1): p. 31-46.
14. Alnaggar, M., et al., *Allogenic Vgamma9Vdelta2 T cell as new potential immunotherapy drug for solid tumor: a case study for cholangiocarcinoma.* J Immunother Cancer, 2019. **7**(1): p. 36.
15. Xiang, Z. and W. Tu, *Dual Face of Vgamma9Vdelta2-T Cells in Tumor Immunology: Anti- versus Pro-Tumoral Activities.* Front Immunol, 2017. **8**: p. 1041.
16. Fisher, J.P., et al., *gammadelta T cells for cancer immunotherapy: A systematic review of clinical trials.* Oncoimmunology, 2014. **3**(1): p. e27572.
17. Gogoi, D. and S.V. Chiplunkar, *Targeting gamma delta T cells for cancer immunotherapy: bench to bedside.* Indian J Med Res, 2013. **138**(5): p. 755-61.
18. Silva-Santos, B., S. Mensurado, and S.B. Coffelt, *gammadelta T cells: pleiotropic immune effectors with therapeutic potential in cancer.* Nat Rev Cancer, 2019. **19**(7): p. 392-404.
19. Ramutton, T., et al., *gammadelta T cells as a potential tool in colon cancer immunotherapy.* Immunotherapy, 2014. **6**(9): p. 989-99.
20. Aggarwal, R., et al., *Human Vgamma2Vdelta2 T cells limit breast cancer growth by modulating cell*

survival-, apoptosis-related molecules and microenvironment in tumors. Int J Cancer, 2013. **133**(9): p. 2133-44.

21. Benzaid, I., et al., *High phosphoantigen levels in bisphosphonate-treated human breast tumors promote Vgamma9Vdelta2 T-cell chemotaxis and cytotoxicity in vivo.* Cancer Res, 2011. **71**(13): p. 4562-72.
22. Meraviglia, S., et al., *In vivo manipulation of Vgamma9Vdelta2 T cells with zoledronate and low-dose interleukin-2 for immunotherapy of advanced breast cancer patients.* Clin Exp Immunol, 2010. **161**(2): p. 290-7.
23. Mattarollo, S.R., et al., *Chemotherapy and zoledronate sensitize solid tumour cells to Vgamma9Vdelta2 T cell cytotoxicity.* Cancer Immunol Immunother, 2007. **56**(8): p. 1285-97.
24. Xiang, Z. and W. Tu, *Dual Face of Vγ9Vδ2-T Cells in Tumor Immunology: Anti- versus Pro-Tumoral Activities.* Frontiers in Immunology 2017. **8**: p. 1-13.
25. Bonneville, M., R.L. O'Brien, and W.K. Born, *Gammadelta T cell effector functions: a blend of innate programming and acquired plasticity.* Nat Rev Immunol, 2010. **10**(7): p. 467-78.
26. Sebestyen, Z., et al., *Translating gammadelta (gammadelta) T cells and their receptors into cancer cell therapies.* Nat Rev Drug Discov, 2020. **19**(3): p. 169-184.
27. Hu, Y., et al., *Selenium nanoparticles as new strategy to potentiate gammadelta T cell anti-tumor cytotoxicity through upregulation of tubulin-alpha acetylation.* Biomaterials, 2019. **222**: p. 119397.
28. Kouakanou, L., et al., *Vitamin C promotes the proliferation and effector functions of human gammadelta T cells.* Cell Mol Immunol, 2019.
29. Wu, Y., R.C. Sims, and A. Zhou, *AFM resolves effects of ethambutol on nanomechanics and nanostructures of single dividing mycobacteria in real-time.* Physical Chemistry Chemical Physics, 2014. **16**: p. 19156-19164
30. Wu, Y.Z., et al., *BRMS1 expression alters the ultrastructural, biomechanical and biochemical properties of MDA-MB-435 human breast carcinoma cells: An AFM and Raman microspectroscopy study.* Cancer Letters, 2010. **293**(1): p. 82-91.
31. Wu, Y.Z. and A.H. Zhou, *In situ, real-time tracking of cell wall topography and nanomechanics of antimycobacterial drugs treated Mycobacterium JLS using atomic force microscopy.* Chemical Communications, 2009(45): p. 7021-7023.
32. McEwen, G.D., et al., *Subcellular spectroscopic markers, topography and nanomechanics of human lung cancer and breast cancer cells examined by combined confocal Raman microspectroscopy and atomic force microscopy.* The Analyst, 2013. **138**: p. 787-797.
33. Wu, Y.Z., et al., *The Analysis of Morphological Distortion During AFM Study of Cells.* Scanning, 2008. **30**(5): p. 426-432.
34. Wu, Y.Z., et al., *Time-dependent surface adhesive force and morphology of RBC measured by AFM.* Micron, 2009. **40**(3): p. 359-364.
35. Wu, Y.Z., et al., *Atomic force microscope tracking observation of Chinese hamster ovary cell mitosis.* Micron, 2006. **37**(2): p. 139-145.
36. Kumari, S., et al., *Reactive Oxygen Species: A Key Constituent in Cancer Survival.* Biomark Insights, 2018. **13**: p. 1177271918755391.
37. Santos, A.L., S. Sinha, and A.B. Lindner, *The Good, the Bad, and the Ugly of ROS: New Insights on Aging and Aging-Related Diseases from Eukaryotic and Prokaryotic Model Organisms.* Oxid Med Cell Longev, 2018. **2018**: p. 1941285.
38. Vucetic, M., et al., *The Central Role of Amino Acids in Cancer Redox Homeostasis: Vulnerability Points of the Cancer Redox Code.* Front Oncol, 2017. **7**: p. 319.